AIP | Applied Physics Letters

Ambipolar doping in SnO

J. B. Varley, A. Schleife, A. Janotti, and C. G. Van de Walle

Citation: Applied Physics Letters **103**, 082118 (2013); doi: 10.1063/1.4819068
View online: http://dx.doi.org/10.1063/1.4819068
View Table of Contents: http://scitation.aip.org/content/aip/journal/apl/103/8?ver=pdfcov
Published by the AIP Publishing

Ambipolar doping in SnO

J. B. Varley,[1,2] A. Schleife,[2] A. Janotti,[1] and C. G. Van de Walle[1]
[1]*Materials Department, University of California, Santa Barbara, California 93106-5050, USA*
[2]*Lawrence Livermore National Laboratory, Livermore, California 94550, USA*

(Received 3 July 2013; accepted 7 August 2013; published online 23 August 2013)

SnO is a promising oxide semiconductor that can be doped both *p*- and *n*-type, but the doping mechanisms remain poorly understood. Using hybrid functionals, we find that native defects cannot account for the unintentional *p*-type conductivity. Sn vacancies are shallow acceptors, but they have high formation energies and are unlikely to form. Unintentional impurities offer a more likely explanation for *p*-type doping; hydrogen is a likely candidate, and we find that it forms shallow-acceptor complexes with Sn vacancies. We also demonstrate that the ambipolar behavior of SnO can be attributed to the high position of the valence-band on an absolute energy scale.
 [http://dx.doi.org/10.1063/1.4819068]

Tin(II) oxide (SnO) has received a great deal of attention ever since ambipolar doping was reported.[1] It is one of the rare oxide semiconductors in which *p*-*n* junctions may be achieved, thus enabling novel electronic and optoelectronic applications.[1–5] Its behavior is in stark contrast to SnO_2, for which only *n*-type conductivity has been realized.[6,7] While *n*-type SnO has been achieved via extrinsic doping with Sb,[1] the observed *p*-type conductivity was achieved without intentional doping, and its microscopic origins have not yet been resolved. Density functional calculations using the generalized gradient approximation (GGA) have indicated that the Sn vacancy (V_{Sn}) acts as a shallow acceptor,[8,9] and this has been indirectly supported by experiments which find that the *p*-type conductivity is enhanced with lower Sn-to-O ratios during growth.[4,5] However, if Sn vacancies were the cause of the observed *p*-type conductivity, it would be very difficult to explain the possibility of *n*-type doping, since the vacancies would be present in even higher concentrations than in *p*-type material and lead to self-compensation. With regard to doping, in contrast to the *n*-type behavior observed by Hosono *et al.*,[1] Guo *et al.* claimed that Sb doping enhances the *p*-type conductivity.[4] These conflicting results highlight the need for further study to address the role of native defects and impurities in doping of this highly promising oxide semiconductor.

We investigate the electronic structure and defect physics of SnO using density functional theory (DFT), but in an implementation (employing hybrid functionals) that does not suffer from the underestimation of the band gap inherent in traditional DFT calculations using the local density approximation (LDA) or GGA. We first discuss the band structure of SnO, later comparing the character of the valence- and conduction-band edges to SnO_2. We then describe the electronic and structural properties of native defects and hydrogen impurities in SnO. We find that the V_{Sn} indeed acts as a shallow acceptor but has a very high formation energy in *p*-type SnO, thus rendering its incorporation highly unlikely. The O interstitial (O_i) is stable exclusively in the neutral charge state and thus cannot contribute to the conductivity. The O vacancy (V_O) is a deep donor, existing in the neutral charge state in *n*-type and 2+ charge state in *p*-type SnO. We also investigate hydrogen impurities, which are likely to be unintentionally incorporated due to the ubiquity of hydrogen in growth and processing environments, and the high solubility which we predict based on our calculated energies. We find that hydrogen forms complexes with Sn vacancies, in the process significantly lowering their formation energy. These $V_{Sn} - H$ complexes still act as shallow acceptors, offering an explanation for the observed unintentional *p*-type conductivity. Finally, we explain the behavior of defects in terms of the absolute energy position of the valence- and conduction-band edges of SnO, elucidating why doping can be so different from SnO_2.

The calculations are based on generalized Kohn-Sham theory with the screened hybrid functional of Heyd, Scuseria, and Ernzerhof (HSE)[10] and the projector augmented-wave method as implemented in the VASP code.[11–14] The Hartree-Fock mixing parameter was set to 32%, which reproduces the experimental band gaps of SnO (Ref. 2) [Fig. 1(a)] and SnO_2 (Ref. 15); the resulting structural parameters are also in better agreement with experiment than GGA values (see Table I) and improve the interlayer-distances similar to methods accounting for van der Waals interactions.[16,17] The Sn 4 *d* electrons were treated as core electrons; tests have shown that their explicit inclusion in the valence leads to changes in formation energies of less than 0.1 eV, a conclusion similar to what we found in SnO_2.[15]

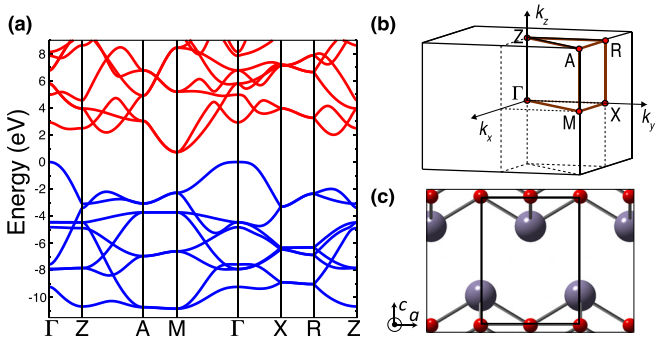

FIG. 1. (a) Band structure of SnO along high-symmetry directions (a), as calculated with the HSE hybrid functional. The gap is indirect with the conduction-band minimum at the M point of the Brillouin zone of the tetragonal SnO unit cell. (b) Brillouin zone of SnO. (c) SnO crystal structure, with the unit cell of the litharge structure outlined. The lattice coordinates *a* and *c* represent the [100] and [001] directions, respectively.

TABLE I. Structural parameters, band gap, and formation enthalpy for SnO, calculated using DFT with either GGA or HSE functionals. Experimental values are listed for comparison.

	a (Å)	c (Å)	u	ΔH_f (eV)	E_g^i (eV)	E_g^d (eV)
GGA	3.860	4.989	0.232	−2.53	0.37	1.93
HSE (32%)	3.784	4.921	0.232	−2.57	0.73	2.93
Expt.	3.799[a]	4.841[a]	0.237[a]	−2.91[b]	∼0.7[c]	∼2.7[c]

[a]Reference 18.
[b]Reference 19.
[c]Reference 2.

For the defect calculations, we used a plane-wave basis set with a cutoff of 400 eV and a 192-atom supercell ($4 \times 4 \times 3$ unit cells), sufficiently large to perform integrations over the Brillouin zone using only the Γ-point. All defect calculations were spin-polarized. Corrections for the Coulomb interaction of charged defects were explicitly included following the scheme described in Refs. 20 and 21, using the weighted spatial-average of the parallel and perpendicular components of the calculated static dielectric constant, $\bar{\varepsilon}_0 = 16.2$. The thermodynamic transition levels for all shallow defects only include a correction that ensures the alignment of the electrostatic potentials in the bulk and defect super cells.[22]

SnO is most stable in the litharge crystal structure, with space-group P4/nmm ($SG129$).[18] In this layered tetragonal structure (shown in Fig. 1(c)), each Sn atom is bonded to four O atoms. The calculated electronic band structure of SnO is shown in Fig. 1(a) and exhibits several notable differences from that of rutile SnO_2, which has been analyzed in detail elsewhere.[15,23] The band gap of SnO is indirect, calculated to be 0.73 eV (Table I). The valence-band maximum (VBM) is located at Γ and the conduction-band minimum (CBM) at the M point [Fig. 1(b)]. The direct gap of 2.93 eV at Γ (3.00 eV at M) is much larger, which allows SnO to remain largely transparent over the visible range (>70%–80% for 100 nm films).[24]

To analyze the role of defects in SnO we calculate defect formation energies (E^f), from which we can derive equilibrium concentrations, and address the stability of different charge states and the related electronic transition levels.[22] For instance, the formation energy of V_{Sn} in SnO is given by

$$E^f[V_{Sn}^q] = E_{tot}[V_{Sn}^q] - E_{tot}[SnO] + \mu_{Sn} + q\varepsilon_F, \qquad (1)$$

where $E_{tot}[V_{Sn}^q]$ and $E_{tot}[SnO]$ represent the total energy of the supercell containing a vacancy in charge state q and that of a perfect crystal in the same supercell. The Sn removed from the crystal is placed in a reservoir with energy μ_{Sn} and the chemical potential of Sn; μ_{Sn} varies depending on the experimental conditions during growth or annealing, ranging from Sn-poor (O-rich) to Sn-rich (O-poor). Limits are set by the stability condition of the solid, i.e., $\mu_{Sn} + \mu_O = \Delta H_f[SnO]$. The Sn-rich limit is taken with respect to solid α-Sn ($\mu_{Sn} = 0$), while the Sn-poor limit is given by the equilibrium condition between SnO and SnO_2. While V_{Sn}-related defects would be lower in energy in the Sn-poor limit, this regime drives the system towards formation of SnO_x ($x > 1$) phases.[25] Therefore in this work we focus on the Sn-rich limit.

For the H impurities and related complexes, we set μ_H to the energy of an H atom in the H_2 molecule at $T = 0$. For antimony, μ_{Sb} is set to the energy of bulk Sb. We also considered competing antimony oxide phases but find that they do not affect μ_{Sb} for conditions in which SnO is stable. Experimentally, different temperature and pressure values will affect μ_H, μ_{Sb}, μ_{Sn}, and μ_O, and such dependences may shift the formation energies, though not by much due to the relatively narrow window of stability of SnO. We note, however, that our reported charge-state transition levels are independent of the choice of chemical potentials. Finally, ε_F in Eq. (1) is the electron chemical potential or Fermi level, conventionally referenced to the VBM.

In Fig. 2(a) we plot the formation energies of the energetically most favorable native defects, as well as hydrogen and antimony impurities in SnO. Consistent with previous reports,[8,9] we find that oxygen interstitials O_i are electrically inactive, occurring in the neutral charge state for all values of Fermi level in the band gap. Oxygen vacancies (V_O) are deep donors with a (2+/0) transition level at 0.24 eV above the VBM. Neither defect can be a source of conductivity, but V_O has low enough formation energy to act as a compensating center in p-type SnO.

The Fermi-level positions at which changes in the charge state occur provide the charge-state transition levels, which can be interpreted as ionization energies. Figure 2(a) shows that the Sn vacancy V_{Sn} has a (0/–) transition level at 0.12 eV and (–/2–) at 0.13 eV above the VBM; these levels are also indicated in Fig. 2(b). V_{Sn} therefore behaves as a double shallow acceptor, consistent with the fact that the defect-induced states (dangling-bond states associated with the four O atoms surrounding the V_{Sn}) are found to lie well below the VBM. The negative and neutral charge states of V_{Sn} therefore correspond to removing electrons from the VBM, and the resulting charge-state transition levels should

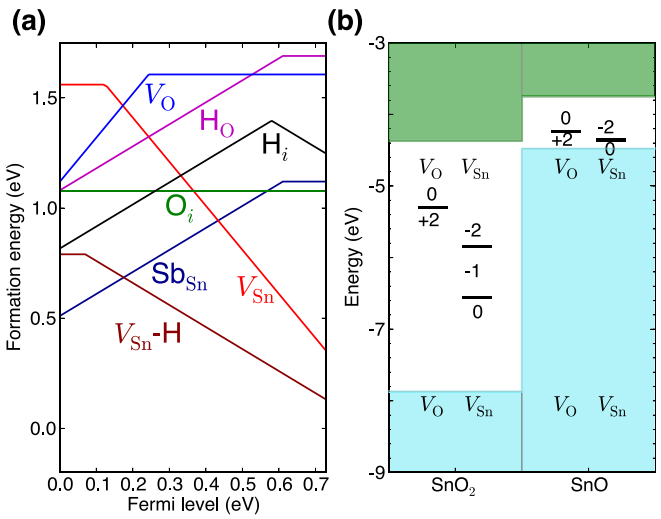

FIG. 2. (a) Formation energy of native point defects as well as Sb and H impurities in SnO. Sn-rich conditions are assumed, as described in the text. (b) Band structures of SnO_2 and SnO relative to the vacuum level. The charge-state transition levels of the native vacancies are indicated within the respective band gaps.

be interpreted in the context of hydrogenic effective-mass theory; they are indeed consistent with estimates of the ionization energies based on dielectric constant and hole effective mass. The latter was calculated to be 2.3 m_e, using a geometric average along the Γ-X (3.2 m_e) and Γ-Z (0.5 m_e) directions.

Figure 2(a) shows that Sn vacancies have a relatively high formation energy in *p*-type SnO, and therefore their concentration will be too low to account for the observed hole concentrations in *p*-type SnO, especially considering the relatively low growth temperatures.[2,5] We note that if V_{Sn} were so prevalent as to be an unintentional source of *p*-type conductivity, they would be even more prevalent in *n*-type material, in which their formation energy is significantly lower [see Fig. 2(a)], and hence self-compensation would occur that would preclude *n*-type doping. The fact that *n*-type doping has proved feasible[1] is a strong indicator that V_{Sn} are not the source of unintentional *p*-type doping.

We therefore attribute the *p*-type conductivity to the unintentional incorporation of impurities, with hydrogen being a prime candidate since it is present in almost all growth and processing environments. We find that interstitial H acts as an amphoteric impurity in SnO, with the (+/–) transition level occurring at 0.15 eV below the CBM for the lowest-energy interstitial configurations [Fig. 2(a)]. In the negative charge state, H_i^- prefers a location in a region of low charge density, as is commonly found in other semiconductors.[26] H_i^+, on the other hand, prefers to bond to a Sn atom, which is different from the behavior in most other oxides.[27,28]

We have also investigated the interaction between hydrogen and vacancies. Hydrogen forms a complex with V_O in which the H atom sits at the center of the vacancy, effectively forming a substitutional impurity H_O. In this configuration, H_O acts as a shallow donor, as shown in Fig. 2(a). Hydrogen also binds strongly with V_{Sn}, forming a complex whose formation energy is much lower than that of isolated V_{Sn} [Fig. 2(a)]. The $V_{Sn}-H$ complex is a shallow acceptor with a (0/–) transition level at 0.07 eV above the VBM, close to the estimated ~100 meV activation energies of shallow acceptors in *p*-type SnO.[1]

The calculated binding energy, defined by $E^f[V_{Sn}^{2-}] + E^f[H_i^+] - E^f[(V_{Sn}-H)^-]$, is 1.92 eV. Such a large binding energy values indicates that the dissociation of $V_{Sn}-H$ complexes would require high temperatures, higher than the temperatures up to which SnO remains stable (~270 °C, Ref. 29). The low formation energy and high binding energy of $V_{Sn}-H$ indicate that these complexes are a likely source of *p*-type conductivity in SnO.

Hydrogen atoms in the $V_{Sn}-H$ complex are bonded to O atoms, resulting in distinct local vibrational modes. To assist in the experimental detection of these complexes in SnO, we calculated the stretch-mode vibrational frequencies, finding frequencies of 3370 cm^{-1} and 3350 cm^{-1} for the 0 and −1 charge states. These results include anharmonic effects as well as systematic corrections as described in Refs. 27 and 30.

Regarding *n*-type conductivity, we report on the behavior of Sb, which we find most favorably incorporates on the Sn site as a shallow donor [Fig. 2(a)]. The calculated ionization energy of 120 meV is close to the ~90 meV shallow donor level reported for Sb-doped SnO.[1] We find that substitutional Sb on the O site and Sb interstitials have much higher formation energies than Sb_{Sn}. In order for Sb_{Sn} to lead to *n*-type doping, compensation by acceptors needs to be avoided; in light of our results above, this requires suppressing hydrogen incorporation, which would lead to $V_{Sn}-H$ acceptors.

Finally, we address why SnO exhibits unintentional *p*-type conductivity and is difficult to dope *n*-type, while SnO_2 exhibits the opposite behavior. An explanation is provided by examining the band alignment between the two compounds. To align the band structures of SnO and SnO_2 on an absolute energy scale we used surface calculations: We first determine the position of the VBM in the bulk with respect to the averaged electrostatic potential, and then, from a slab calculation, we determine the averaged electrostatic potential in a bulk-like region with respect to the vacuum level.[31] Slabs containing 6 unit cells and oriented along the [001] direction were used, separated by an equal thickness of vacuum. Surface relaxations were included for both surfaces, with the atoms in the two innermost unit cells kept fixed at their bulk positions.

The results are shown in Fig. 2(b), indicating a type-II alignment with the VBM of SnO much higher in energy than in SnO_2: the calculated valence-band offset is 3.39 eV. Using an alternative alignment procedure based on the position of the (+/–) transition level of interstitial hydrogen,[26] we find a valence-band offset of 3.51 eV, in excellent agreement with the alignment based on surface calculations. It is interesting to note that the VBM of SnO is just below the CBM of SnO_2, within ~0.1 eV. This can be explained in terms of the differences in the SnO and SnO_2 band structures. Focusing on the band extrema [Fig. 3(a)], the CBM in SnO is degenerate, with its orbital character deriving mostly from Sn *p*

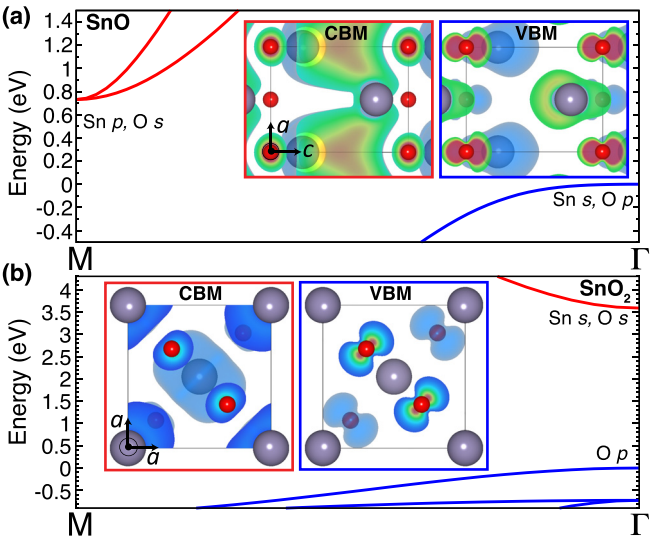

FIG. 3. Dispersion of the highest valence bands and lowest conduction bands near the band extrema in (a) SnO and (b) SnO_2. The insets show the charge-density isosurfaces for the band extrema, displaying distinct differences that underlay the contrasting electronic structure of these two materials. The left inset shows the CBM, while the right inset shows the VBM, with all isosurfaces shown at 10% of their maximum value. The lattice coordinates *a* and *c* represent the [100] and [001] directions, respectively.

states with some contribution from O *s*. This is very different from SnO_2, in which the CBM has mostly Sn *s* character, along with some contribution from O *s* [Fig. 3(b)].

An even more notable difference occurs for the VBM. In SnO, the character of the VBM is derived mostly from Sn *s* states mixed with the O p_z states, consistent with current lone-pair models of this material.[32] In SnO_2, the VBM is derived mostly from the O *p* states, without any Sn *s* contribution. Since the Sn *s* states are significantly higher in energy than the O *p* states,[33] it is to be expected that the VBM in SnO lies at a much higher energy than in rutile SnO_2. In addition, the Sn *p* states are even higher, which suggests the SnO CBM should lie above that of SnO_2, also consistent with our type-II band alignment between SnO and SnO_2. The orbital character of the band edges in SnO and SnO_2 was also discussed by Hosono *et al.*, who noted that the much higher position of the SnO VBM relative to the vacuum level allows *p*-type conductivity in SnO, but not in SnO_2.[1]

In summary, we have performed first-principles calculations to elucidate unintentional and intentional doping in SnO. For native defects, we concluded that while the Sn vacancy is a shallow acceptor, its formation energy is too high to explain the unintentional *p*-type conductivity. Hydrogen, a ubiquitous impurity, can lead to shallow-acceptor defects in the form of $V_{Sn} - H$ complexes. Antimony acts as a shallow donor, incorporating on the Sn site. Band-alignment calculations show that SnO and SnO_2 exhibit a type-II alignment with the CBM of SnO_2 lying very close to the VBM of SnO. These results offer insight into the mechanisms underlying the observed conductivity, confirming that SnO is a promising oxide for ambipolar doping.

Discussions with S. Küfner and F. Bechstedt are gratefully acknowledged. This work was supported by the NSF MRSEC Program (DMR-1121053). Computational resources were provided by the Center for Scientific Computing at the CNSI and MRL (an NSF MRSEC, DMR-1121053) (NSF CNS-0960316) and by the Extreme Science and Engineering Discovery Environment (XSEDE), supported by NSF (OCI-1053575 and DMR07-0072N). Part of this work was performed under the auspices of the U.S. Department of Energy at Lawrence Livermore National Laboratory under Contract No. DE-AC52-07A27344.

[1]H. Hosono, Y. Ogo, H. Yanagi, and T. Kamiya, Electrochem. Solid-State Lett. **14**, H13 (2011).
[2]Y. Ogo, H. Hiramatsu, K. Nomura, H. Yanagi, T. Kamiya, M. Hirano, and H. Hosono, Appl. Phys. Lett. **93**, 032113 (2008).
[3]H. Yabuta, N. Kaji, R. Hayashi, H. Kumomi, K. Nomura, T. Kamiya, M. Hirano, and H. Hosono, Appl. Phys. Lett. **97**, 072111 (2010).
[4]W. Guo, L. Fu, Y. Zhang, K. Zhang, L. Y. Liang, Z. M. Liu, H. T. Cao, and X. Q. Pan, Appl. Phys. Lett. **96**, 042113 (2010).
[5]E. Fortunato, R. Barros, P. Barquinha, V. Figueiredo, S.-H. K. Park, C.-S. Hwang, and R. Martins, Appl. Phys. Lett. **97**, 052105 (2010).
[6]M. E. White, O. Bierwagen, M. Y. Tsai, and J. Speck, Appl. Phys. Express **3**, 051101 (2010).
[7]Z. Ji, L. Zhao, Z. He, Q. Zhou, and C. Chen, Mater. Lett. **60**, 1387 (2006).
[8]A. Togo, F. Oba, I. Tanaka, and K. Tatsumi, Phys. Rev. B **74**, 195128 (2006).
[9]D. B. Granato, J. A. Caraveo-Frescas, H. N. Alshareef, and U. Schwingenschlögl, Appl. Phys. Lett. **102**, 212105 (2013).
[10]J. Heyd, G. E. Scuseria, and M. Ernzerhof, J. Chem. Phys. **124**, 219906 (2006).
[11]G. Kresse and J. Furthmüller, Phys. Rev. B **54**, 11169 (1996).
[12]G. Kresse and D. Joubert, Phys. Rev. B **59**, 1758 (1999).
[13]P. E. Blöchl, Phys. Rev. B **50**, 17953 (1994).
[14]M. Marsman, J. Paier, A. Stroppa, and G. Kresse, J. Phys.: Condens. Matter **20**, 064201 (2008).
[15]J. B. Varley, A. Janotti, and C. G. Van de Walle, Phys. Rev. B **81**, 245216 (2010).
[16]J. P. Allen, D. O. Scanlon, S. C. Parker, and G. W. Watson, J. Phys. Chem. C **115**, 19916 (2011).
[17]K. Govaerts, R. Saniz, B. Partoens, and D. Lamoen, Phys. Rev. B **87**, 235210 (2013).
[18]F. Izumi, J. Solid State Chem. **38**, 381 (1981).
[19]*CRC Handbook of Chemistry and Physics*, edited by D. R. Lide (CRC Press, Boca Raton, FL, 2005), pp. 850–856.
[20]C. Freysoldt, J. Neugebauer, and C. G. Van de Walle, Phys. Rev. Lett. **102**, 016402 (2009).
[21]C. Freysoldt, J. Neugebauer, and C. G. Van de Walle, Phys. Status Solidi B **248**, 1067 (2011).
[22]C. G. Van de Walle and J. Neugebauer, J. Appl. Phys. **95**, 3851 (2004).
[23]A. Schleife, J. B. Varley, F. Fuchs, C. Rödl, F. Bechstedt, P. Rinke, A. Janotti, and C. G. Van de Walle, Phys. Rev. B **83**, 035116 (2011).
[24]H.-N. Lee, H.-J. Kim, and C.-K. Kim, Jpn. J. Appl. Phys. **49**, 020202 (2010).
[25]A. Seko, A. Togo, F. Oba, and I. Tanaka, Phys. Rev. Lett. **100**, 045702 (2008).
[26]C. G. Van de Walle and J. Neugebauer, Nature (London) **423**, 626 (2003).
[27]J. B. Varley, H. Peelaers, A. Janotti, and C. G. Van de Walle, J. Phys.: Condens. Matter **23**, 334212 (2011).
[28]K. Xiong, J. Robertson, and S. J. Clark, J. Appl. Phys. **102**, 083710 (2007).
[29]G. H. Moh, Chem. Erde **33**, 243 (1974).
[30]W. M. H. Oo, S. Tabatabaei, M. D. McCluskey, J. B. Varley, A. Janotti, and C. G. Van de Walle, Phys. Rev. B **82**, 193201 (2010).
[31]P. G. Moses, M. Miao, Q. Yan, and C. G. Van de Walle, J. Chem. Phys. **134**, 084703 (2011).
[32]A. Walsh, D. J. Payne, R. G. Egdell, and G. W. Watson, Chem. Soc. Rev. **40**, 4455 (2011).
[33]W. Harrison, *Electronic Structure and the Properties of Solids* (Dover, Mineola, NY, 1989).